Journal of Applied Mechanics Vol.11, pp.735-743 (August 2008) JSCE

3-D Flood Flow Structures in a Doubly Meandering Compound Channel under Dominant Relative Depth

G.M. Tarekul Islam *, Yoshihisa Kawahara ** and Nobuyuki Tamai***

* Member, PhD, Visiting Researcher, Division of Social and Envrn. Eng., Graduate School of Eng., Hiroshima University (1-4-1 Kagamiyama, Higashi-Hiroshima, Hiroshima 739-8527)
**Member, Dr. of Eng., Professor, Division of Social and Envrn. Eng., Graduate School of Eng., Hiroshima University (1-4-1 Kagamiyama, Higashi-Hiroshima, Hiroshima 739-8527)
***Member, Dr. of Eng., Professor, Graduate School, Kanazawa Gakuin University (Sue-Machi 10, Kanazawa, Ishikawa 920-1392)

A doubly meandering compound channel is one in which both lower and upper channel meander. This paper examines the 3-D flood flow structures in terms of primary velocity distribution, stream-wise velocity distribution and secondary currents in a doubly meandering compound channel under dominant relative depth. The relative depth is the ratio of the depth of water over the floodplain to the total depth of water while the dominant relative depth is the relative depth at which the difference in discharge between the rising and falling stages takes the maximum value. The dominant relative depth of a doubly meandering compound channel is found to be 0.17. The primary velocity distribution under the dominant relative depth appears to be essentially the same for both rising and falling stages. The exchange of flow between main channel and floodplain results in the retardation and deviation of flow fields. The extent of retardation and the angle of deviation of the stream-wise velocity vary in the rising and falling stages. The maximum retardation occurs in the cross-over section at the floodplain level for both rising and falling stages. The maximum deviation occurs at the bend apex section for both rising and falling stages. The magnitude of the secondary current under dominant relative depth can be as high as 30% of the bulk velocity. The evolution and decay processes of secondary currents during rising and falling stages are essentially the same but only differ in strength.

Key Words: *3-D structure; flood flow; doubly meandering; compound channel; relative depth*

1. Introduction

A natural meander river is usually composed of a deep main channel and adjacent shallow floodplains. Such compound channels offer advantages mainly that of ensuring reasonable depth at low flows, while the floodplains give storage for floods during high flows. This is why a two-stage channel or compound channel is proposed as a design cross-section to retain large parts of the natural environment unchanged. When the main meander channel is flanked by floodplains with meandering levee, it results in a doubly meandering compound channel. The surrounding lands of the floodplain might compel one to construct meandering levees. In addition, the alignment of the meandering levees might be of special interest as far as maintenance of the channel is concerned. For a particular levee alignment, the flow structures might be such that it requires less maintenance for bank protection and other works. Here lies the engineering significance of a doubly meandering compound channel. The flow structure is complex even for straight compound channel. It has been pointed out that at a low floodplain depth the large velocity difference between the main channel and the floodplain induces a strong shear layer and a lateral momentum transfer across the interface between the main channel and the floodplain[1,2]. The flow mechanisms are more complex for meandering compound channel due to an increase in the three-dimensional nature of the flow, the interaction between the flows in the main channel and the floodplain and the unsteady nature of flow.

In natural rivers, most of the flows are unsteady especially

during flood. The unsteadiness of the flood waves influences the velocity distribution, suspended sediment transport, bed load sediment transport etc.[3]. Many investigations have been conducted to understand the unsteady flow characteristics in straight single section channel and straight compound channel. Tu and Graf[4] studied the velocity distribution in unsteady open-channel flow and they obtained the friction velocity as well as the shear-stress distribution by using the kinematic wave theory. Nezu et al.[5] investigated the effects of unsteadiness on velocity profiles over rough beds in flood surface flow and found that the unsteadiness effects on the π-parameter in the log-wake law differ significantly from those on the friction velocity and bed shear stress. Tominaga et al.[6] experimentally investigated the hydraulic characteristics of unsteady flow in compound channels with vegetated floodplains. They found that the vegetation in the floodplains increases the unsteadiness of the main channel velocity and its double peak property of the depth-averaged velocity in the main channel is changed by the effects of vegetation arrangement. Jayaratne et al.[7] studied the unsteady flow characteristics of a meandering compound channel and found that the velocity reaches its maximum first followed by discharge and water depth. Lai et al.[8] conducted experiments on flood-wave propagation in a meandering compound channel. They studied flood waves based on three features, i.e., the hydrograph shape, the overbank wave front, and the stage-velocity relations. Fukuoka et al.[9] studied the effects of unsteadiness, planform and cross-sectional form of channel on hydraulic characteristics of flood flow. Morishita et al.[10] studied flood flow structures during rising and falling stages in a compound meandering channel. They found that the convective momentum transfer in the vertical direction is more active during rising stage than during falling stage. This paper explores the 3-D flood flow structure in a doubly meandering compound channel under dominant relative depth.

2. Experimental Setup and Measurement

The experiments were conducted in a tilting flume whose length, width and depth are 30 m, 1.5 m and 1 m, respectively. The flume, constructed with vinyl chloride, was mounted on 2 m wide steel channel structures. Fig. 1 shows the general layout of the experimental channel. The longitudinal gradient of the channel is adjustable with a jack and hinge and can be varied up to 5%. The channel consists of a main channel flanked by meandering levees on both sides of the main channel. The outer levee which has the same sinuosity as that of main meander channel has a phase difference of about 30^0 ahead of main channel. The meanders are expressed as combinations of arcs and straight reaches. The flume consists of nine consecutive meandering waves with straight approach channels at the beginning and end of the meandering part of the channel. The bed of the main channel and floodplains is smooth. The width and depth of the main channel are 300 mm and 50 mm, respectively. The angle of arc is 60^0 with a sinuosity of 1.05. The water supply system in the channel is a closed one. From the downstream reservoir the water is transported by means of pipeline to the upstream reservoir. Consequently it flows to the experimental model and returns to the underground sump. Two approach channels (length = 2.75 m) have been placed at the beginning and end of the meandering compound channel. The approach channel is a straight compound channel having a main channel of cross-section of 0.30 m × 0.05 m which is flanked by floodplain on both sides. This channel connects the meandering compound channel smoothly so that the flow can enter the main meandering channel without disturbance. Similarly the approach channel at the end provides smooth exit of the outgoing flow to the downstream reservoir through the end of the channel.

For the study of the flow in a doubly meandering compound channel, the relationship between the alignment of the main channel and the levee is of great importance. The phase shift is defined as the difference between peak of the main channel bend and that of the floodplain in the longitudinal direction. More precisely, the phase shift is the ratio of the difference between the peak of the main channel bend and that of the meander flood levee to the wave length. The phase shift can be either positive or negative depending on the position of the meander levee. If the apex of the meander levee lies ahead of the bend apex of the main channel, then it is said to have a positive phase shift and vice versa. The phase shift of this doubly meandering compound channel is about 30^0 ahead of the main channel. Fig. 2 shows the definition sketch of different geometric parameters. The magnitudes of different geometric parameters are shown in Table 1.

For the measurement of water levels and velocities, the measuring probes were mounted on a carriage which traveled along the flume on a rail system. The movement of the carriage in the transverse and vertical direction is automatically performed by electric motor which can be programmed to move the probe to the desired position. The 3-D point velocities were measured by two sets of two-component electromagnetic current meters viz. I- and L-type probes (Kenek Company, Japan). The I-type probe was used for measuring x- and y-velocity components while the L-type probe was used for z-velocity component. The x-velocity is in the direction normal to each cross section, y-velocity is in the direction parallel to the cross section and z-velocity is in the vertical direction. The sampling frequency of the current meter was 5 Hz. An electromagnetic flow meter installed in the outflow pipe was used to measure the instantaneous discharge. The sampling frequency of discharge measurement was 1 Hz. The electromagnetic current meters and flow meter were connected to an A/D (Analog/Digital) convertor. The A/D convertor board was then connected to a personal computer for automatic data acquisition.

As the main channel meander is regular, the flow field is considered to be the same at positions in phase after the flow is fully developed. Thus the measuring reach has been selected at a distance of about 15 m from the beginning of the meander channel so as to ensure fully developed flow condition. The velocity in five sections

has been measured in the meander reach covering half of the meander wave (Fig. 3). Sections 1 and 5 are bend apex sections while section 3 is the cross-over section. The measuring grid in the transverse direction was kept fine at the interface and coarse far from the interface. The transverse grid spacing in the main channel is 1 cm from the interface which is followed by 2 cm and 4 cm until the centerline of the section. The transverse grid spacing in the floodplains is 3 cm from the interface which is followed by 8 cm. The grid spacing in the vertical direction is 1 cm from the main channel bed up to 3 cm and then followed by 2 cm. The sectional view of the measuring grid is shown in Fig. 4.

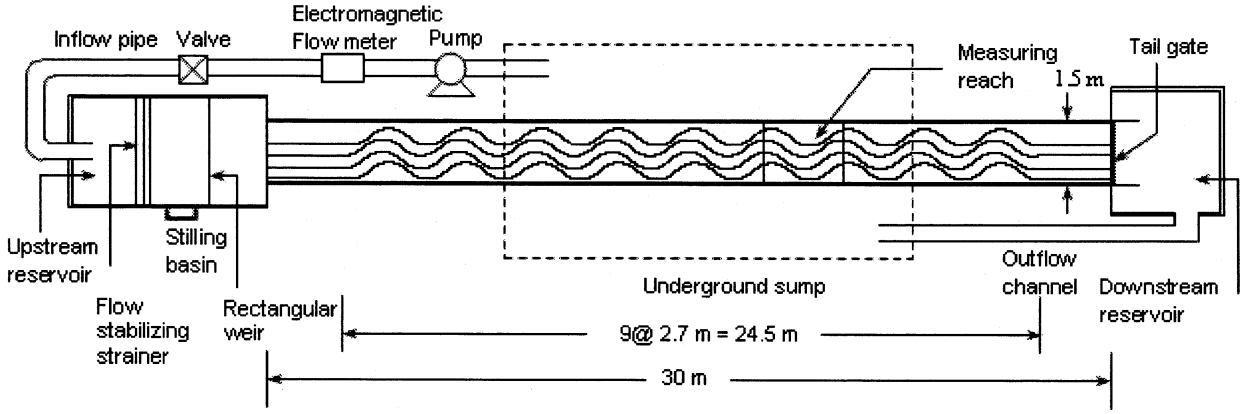

Fig. 1 General layout of the experimental setup

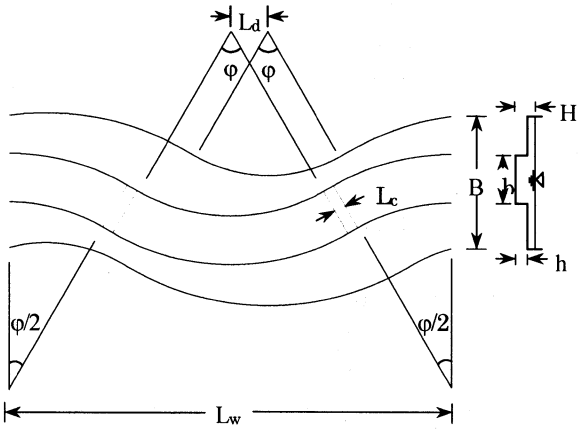

Fig.2 Definition sketch of the geometric parameters

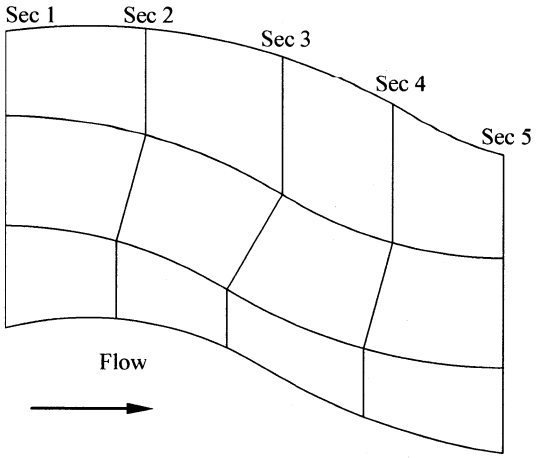

Fig. 3 Measuring reach and sections

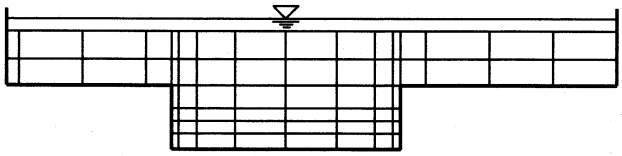

Fig. 4 Sectional (section 1) view of measuring grid

Table 1 Geometric parameters of the compound meandering channel

Parameters	Dimension
Meander wavelength	$L_w = 2.720$ m
Curved channel length	$L = 2.863$ m
Cross-over length	$L_c = 0.070$ m
Phase difference	$L_d = 0.229$ m
Total width	$B = 0.800$ m
Channel width	$b = 0.300$ m
Height of floodplain	$h = 0.050$ m
Sinuosity	$S = 1.05$
Angle of arc	$\varphi = 60^0$
Main channel inner radius	$R_{mi} = 1.150$ m
Main channel outer radius	$R_{mo} = 1.450$ m
Flood levee inner radius	$R_{fi} = 0.900$ m
Flood levee outer radius	$R_{fo} = 1.700$ m

3. Unsteadiness Parameter

It is necessary to define an unsteadiness parameter that characterizes the effects on velocity profiles and turbulence in flood surface flows. The overall characteristics of a hydrograph can be expressed by an unsteadiness parameter. Nezu and Nakagawa (1993) defined a parameter, α to express unsteadiness:

$$\alpha = V_s / U_c \tag{1}$$

The unsteadiness parameter, α is the ratio of the rising speed V_s of flood water surface to the convection velocity U_c of turbulent

eddies.

Graf and Suszka[11] proposed an unsteadiness parameter to express the overall characteristics of a hydrograph. The parameter is:

$$\Gamma_{HG} = \frac{1}{u_b^*}\frac{\Delta D}{\Delta T} \tag{2}$$

where u_b^* = friction of the base flow (before the passage of the hydrograph); ΔD = difference between the maximum flow depth and the base flow depth; and ΔT = total time duration of the hydrograph.

In this study, the following parameter has been used to express the unsteadiness:

$$\sigma = \sqrt{-\left(\frac{\partial^2 H}{\partial t^2}\right)_{t=0} g} \Big/ i \tag{3}$$

where $\left(\frac{\partial^2 H}{\partial t^2}\right)_{t=0}$ represents the curvature of the hydrograph near the origin of time, g is the gravitational acceleration, i is the longitudinal bed slope of the channel. The physical significance of the parameter is that it relates vertical acceleration of water level to the gravitational acceleration. In this study, the above parameter as expressed by Eq. (3) has been used to express the unsteadiness.

4. Selection of Hydrograph

A hydrograph consists of base flow, rising limb, peak and falling limb which is followed by base flow. Different components of a hydrograph are schematically shown in Fig. 5. The notations in the Figure are: H = water depth in a hydrograph; ΔT = total time duration of the hydrograph; ΔT_r = time duration of the rising branch of the hydrograph; ΔT_f = time duration of the falling branch of the hydrograph; H_{base} = water depth of the base flow before passage of the hydrograph; H_{peak} = water depth corresponding to the peak flow; $\Delta H = H_{peak} - H_{base}$.

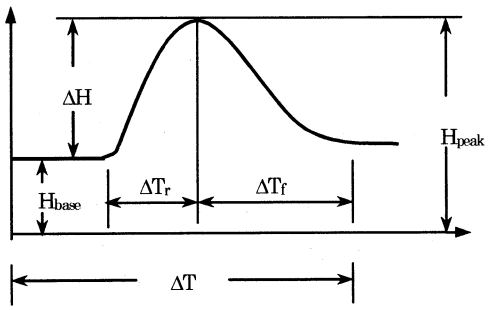

Fig. 5 Schematic representation of a hydrograph

Islam[12] studied natural hydrographs and found that the natural hydrographs and found that a hydrograph usually take a skewed shape with water level first increasing rapidly in the rising branch and then decreasing slowly in the falling branch. The water depth (or discharge) reaches its maximum value at about one third of the total duration of the hydrograph. The unsteadiness parameter varies from 1×10^{-2} - 6×10^{-2}. Keeping these in mind, the hydrograph was selected in such a way that at the beginning, steady flow was maintained by a constant discharge as base flow for 10 minutes. Then it was gradually increased to a peak value in 30 minutes. Then the flow was decreased gradually to reach its base flow in 62 minutes. The different parameters for the selected hydrograph are as follows: $\Delta T_f/\Delta T = 1/3$; $\Delta Q/\Delta T_r = 1.14\times10^{-4}$ m^3/s^2, where ΔQ is the difference between peak flow and base flow; $\sigma = 4.33\times10^{-2}$. The unsteady flow hydrograph was generated by using a software which consists of two parts. One is data logging software used for automatic logging of data while the other is unsteady flow generating software used for generating unsteady flow. One of the difficult aspects to study unsteady flow is how to separate the mean-velocity component, $\bar{u}(t)$ from the instantaneous velocity, $\bar{u}(t) + u'(t)$. In this study, moving average method has been applied. In order to obtain the time dependent flow fields, the velocity signals were arranged in time so as to be $t = 0$ at the rising point of the hydrograph. Then the time was divided into consecutive 5 second-period and the velocities were averaged in each period.

5. Dominant Relative Depth

Fig. 6 shows the discharge and water depth (section 1) hydrographs. It is seen that the peak of discharge is followed by the peak of water depth. This is attributed to the fact that discharge data corresponds to the one as measured by the electromagnetic flow meter installed in the delivery pipe. It is also seen that the rate of rise of water level is faster in the initial stage than that of discharge while the rate of fall of water level is slower than that of discharge. This can be attributed to the cross-sectional shape of the channel.

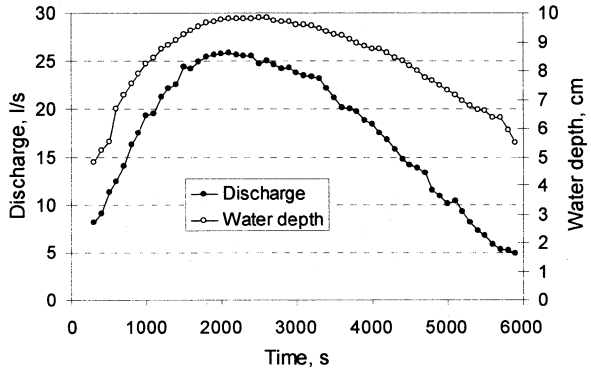

Fig. 6 Hydrographs of discharge (in the delivery pipe) and water depth (section 1)

The relative depth, Dr is defined as the ratio of the depth of water over the floodplain to the total depth of water. Fig. 7 shows

the variation of discharge with relative depth. The relative depth as shown in Fig. 7 has been based on the average water depth in the transverse direction in section 1. As can be seen that the discharge and relative depth relationship is highly non-linear and characterized by the familiar clock-wise loop formation. The difference in discharge between the rising and falling stage takes the maximum value at a relative depth of 0.17 and then gradually narrows down to zero at the peak water depth. This suggests that the difference of flow characteristics in the rising and falling stages is distinctive at a relative depth of 0.17. Hence the 'dominant relative depth' can be defined as the relative depth at which the difference in discharge between the rising and falling stages takes the maximum value. The times needed to attain the dominant relative depth for both rising and falling stages are 160 and 5420 seconds, respectively. It can be concluded that the dominant relative depth of a doubly meandering compound channel under the given flow condition is 0.17. This finding is different from the study of Morishita et al.[11] which involved meandering compound channel with straight floodway. They found that the difference in discharge in the rising and falling stage takes the maximum value at a relative depth of 0.30.

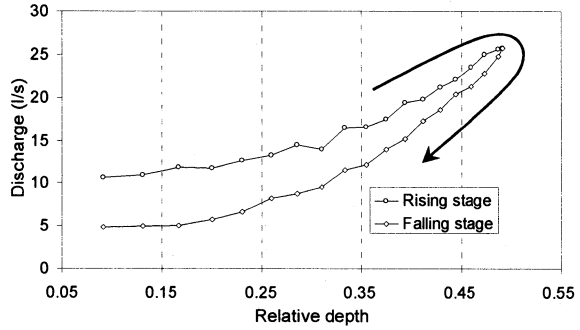

Fig. 7 Variation of discharge with relative depth

6. Primary Velocity Distribution

Figs. 8 to 12 show the primary velocity distribution for rising and falling stages under dominant relative depth at sections 1 to 5, respectively. The primary velocity (u) has been made dimensionless by dividing it with the bulk velocity at section 1 (Ub1). The vertical (z) and lateral distances (y) have been made dimensionless by dividing with the height of floodplain (h). It is seen that the magnitudes of primary velocity fields are higher in case of rising stage than falling stage at all the sections. At section 1, it is seen that the maximum velocity field lies near water surface of the right bank while the minimum velocity field lies near bed of the left bank for both rising and falling stages. The velocity contours are almost evenly spaced except near the right bank where the contours are a bit closely-spaced. A core of high velocity field appears to evolve near the bed at the right bank and becomes fully developed at the cross-over region section. At section 2, the closely-spaced contours in the right bank extend in the lateral direction. The maximum velocity field still lies near the surface but shifts towards the left bank. The evenly-spaced contours spread over the two-third of the cross-section whereas the contours in the remaining part of the section are rather densely-spaced representing high velocity gradients over that region. In the cross-over section, the maximum velocity field continues to move further towards the left bank. Before reaching the next bend apex, both maximum and minimum velocity contours lie near the water surface: the maximum being at the left bank while the minimum near the middle of the cross-section. At section 5, the shift of maximum velocity field ceases and starts to move in the right bank. It is observed that the primary velocity contour in the bend apex section is more or less uniformly distributed which implies that the velocity gradients are low. Further downstream at the cross-over region, the uniformity of velocity distribution is reduced which implies that the velocity gradients across the section is higher than that in the previous section. This is due to the exchange of flow between main channel and floodplain. The flow from right floodplain impinges in the main channel which in turn causes the primary velocity vectors to retard. This retardation is maximum at the cross-over section as can be seen in the contour plots. The primary velocity distribution and the extent of retardation due to momentum exchange appear to be essentially the same for both rising and falling stages under dominant relative depth.

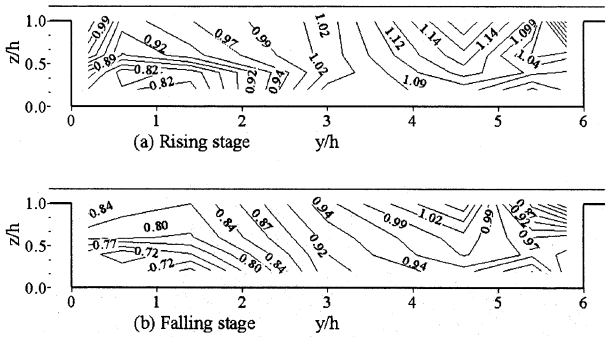

Fig. 8 Primary velocity (u/U_{b1}) distribution at section 1

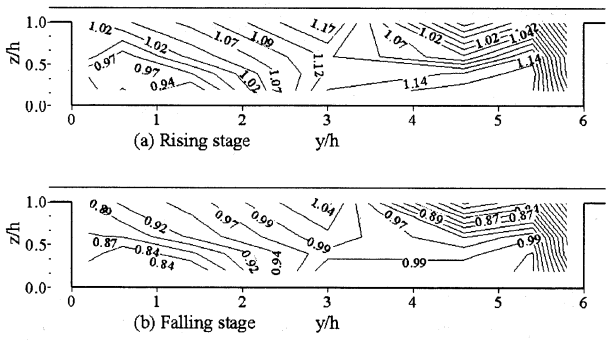

Fig. 9 Primary velocity (u/U_{b1}) distribution at section 2

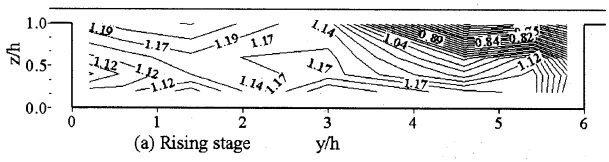

Fig. 10 Primary velocity (u/U_{b1}) distribution at section 3

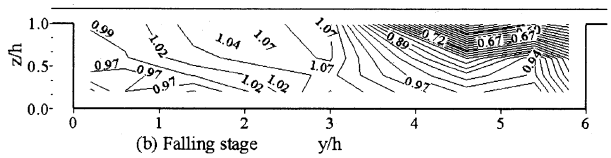

Fig. 10 Primary velocity (u/U_{bl}) distribution at section 3 (*Continued*)

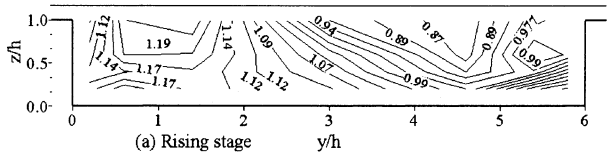

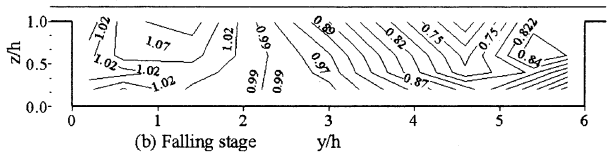

Fig. 11 Primary velocity (u/U_{bl}) distribution at section 4

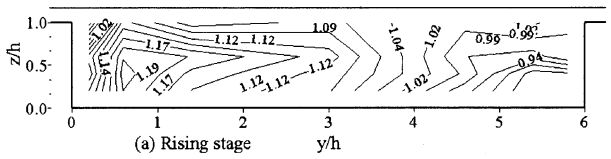

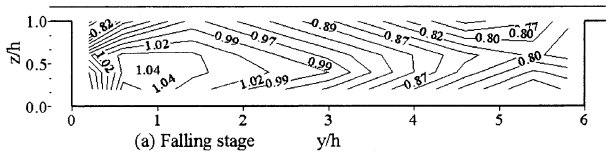

Fig. 12 Primary velocity (u/U_{bl}) distribution at section 5

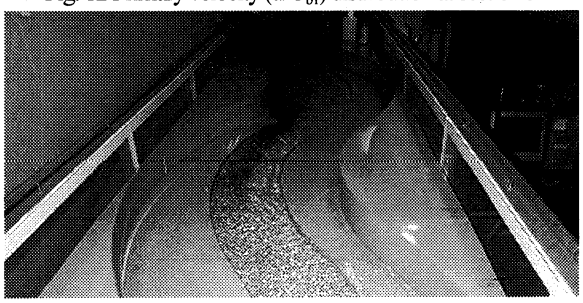

Fig. 13 Flow visualization showing how flow from floodplain impinges main channel

7. Stream-wise Velocity Distribution

Fig. 14 shows the stream-wise velocity distribution at the dominant relative depths in the rising and falling stages, respectively. The stream-wise velocity is the resultant of the x-velocity (u) and the y-velocity (v). It is seen that the magnitude of velocity fields is higher in case of rising stage than that of falling stage. At section 1, the maximum velocity occurs near the right bank while the minimum velocity occurs near the left bank for both rising and falling stages. Following the bend apex section at section 2, the stream-wise velocity fields show that the maximum velocity occurs near right bank of the main channel while the minimum velocity occurs near the left bank for both rising and falling stages. The stream-wise velocity fields in the cross-over section follow the alignment of the main channel. This means that the flow fields are perpendicular to the section at the point of inflection where the curvature effect is non-existent. Following the cross-over region at section 4, it can be seen that the maximum velocity occurs near the left bank while the minimum velocity occurs near the right bank for both rising and falling stages.

It is seen that the stream-wise velocity pattern near main channel bed is the same for both rising and falling stages. The stream-wise velocity fields near main channel bed follow the main channel alignment. The transverse profiles of the flow fields are regular near the channel bed. At higher depths, the transverse profiles lose its regularity and their irregularity becomes more pronounced for both rising and falling stages. This suggests that the effect of the exchange of momentum between main channel and floodplain is less near the channel bottom for both rising and falling stages. The difference in magnitude of the stream-wise velocities for a particular section near main channel bed is high at the bend apex section and low at the cross-over section for both rising and falling stages. At the floodplain height, the difference in magnitudes of the stream-wise velocities is high at the cross-over section and low at the bend apex as opposed to the case near the main channel bed.

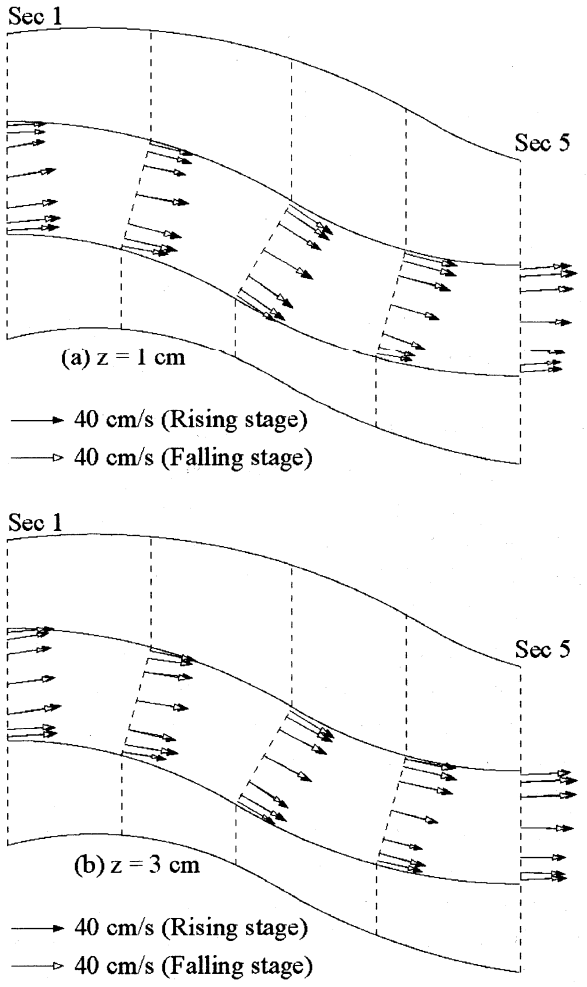

Fig. 14 Transverse distribution of stream-wise velocity

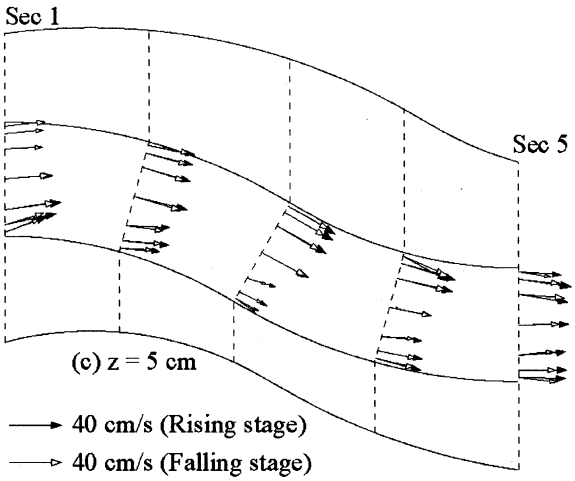

Fig. 14 Transverse distribution of stream-wise velocity (*Continued*)

The exchange of momentum between main channel and floodplain causes the stream-wise velocity to deviate from floodplain towards main channel and from main channel towards floodplain. It is seen that the deviation of the stream-wise velocity increases at higher depth and becomes maximum at the floodplain level which is subject to severe interaction between main channel and floodplain. The exchange of flow between main channel and floodplain results in the retardation of flow fields. The flow from right floodplain impinges in the main channel (Fig. 13) which in turn causes the velocity vectors to retard and deviate. As the retardation of stream-wise velocity arises due to the exchange of flow between main channel and floodplain, it is estimated by comparing to the stream-wise velocity near channel bed. The maximum retardation occurs in the cross-over section at the floodplain level for both rising and falling stages. In order to have a closer look, the retardation and deviation of the stream-wise velocity at right bank for sections 1 and 3 are analyzed. Table 2 shows the magnitude of the stream-wise velocity and the angle of deviation at right bank for dominant relative depth during rising and falling stages and for the bend apex (section 1) and cross-over (section 3) sections at depths of 5 cm and 1 cm which correspond to floodplain level and near channel bed, respectively.

Table 2 Magnitude of stream-wise velocity, V (m/s) and angle of deviation, θ(degree)

Section	z, cm	Rising stage		Falling stage	
		V	θ	V	θ
Bend apex (Section 1)	1	39.2	1.7	32.7	1.8
	5	31.2	10.2	26.4	10.5
Cross-over (Section 3)	1	35.0	-2.3	30.9	-2.0
	5	20.1	0.3	17.5	-2.9

It is found that the extent of retardation of stream-wise velocity at section 1 is higher in the rising stage than that in the falling stage while at section 3 it is higher in the falling stage than that in the rising stage. The angle of deviation is measured with respect to a line perpendicular to the measuring section. It can be seen that the angle of deviation of the stream-wise velocity in the bend apex section is towards the left bank and is higher in the falling stage than that of the rising stage. The angle of deviation of the stream-wise velocity in the cross-over section is towards the right bank near channel bed for both rising and falling stages while at the floodplain height, it is towards the left bank for the rising stage and towards the right bank for the falling stage. It is also seen that the deviation is higher in the rising stage than that of the falling stage near channel bed while it is higher in the falling stage than that of the rising stage at floodplain height. The maximum deviation occurs at the bend apex section for both rising and falling stages.

8. Secondary Currents

Turbulent flow in a compound channel is characterized by a shear layer generated by the velocity between the main channel and the floodplain flow. In this region, there are not only vortices with vertical axis but also those with longitudinal axis. The latter is known as the secondary currents. Secondary currents are defined as currents which occur in the plane normal to the local axis of the primary velocity. It is one of the physical mechanisms by which linear momentum is transferred perpendicular to the direction of the flow. They are important in that they distort the distribution of primary velocities and boundary shear stress from those expected in simple section flow and thus affect the processes of flow resistance, sediment transport, bed and bank erosion and influence the development of channel morphology. The secondary flow cell in single meandering channel occurs mainly due to the action of centrifugal forces. However, when there is flow over the floodplain in a compound meandering channel the interchange of flow between main channel and floodplain gives rise to a different type of secondary flow.

Figs. 15 to 19 show the secondary flow structures in sections 1 to 5, respectively during rising and falling stage under dominant relative depth. The vertical (z) and lateral distances (y) have been made dimensionless by dividing with the height of floodplain (h). At section 1, the overall direction of secondary flow is from right to left floodplain for both rising and falling stages. The magnitude of the secondary current at section 1 is in the order of more than 30% of the bulk velocity. The secondary flow from right floodplain enters the main channel and from main channel to left floodplain. This means that the momentum is transferred from right floodplain to main channel and from main channel to left floodplain. The transfer of momentum along with the centrifugal force drives a clockwise cell to develop near water surface in the left bank of the main channel. Two small anticlockwise cells appear to develop at both the corners of the main channel for both rising and falling stages. The mechanism of the development of secondary cell during falling stages is similar to that of the rising stage. The difference is that the magnitudes of the flow components are larger during rising stage than that during falling stage. As the flow approaches from

section 1 to section 2, it is seen that the overall direction of secondary flow is still from right to left. The clockwise cell developed near water surface in section 1 continues to grow. The anticlockwise cells in the corners grow in size for both rising and falling stages. As the flow goes down from section 2 to section 3 (cross-over), the secondary flow is dominated by the vertical components. The clockwise cell near water surface disappears. The anticlockwise cells in the two sides of the main channel develop further for both rising and falling stages. At section 4, the anticlockwise cell in the main channel near bed of the left bank completely disappears. The other anticlockwise cell in the main channel near bed of the right bank grows and the extent of the cell is from channel bed to the water surface. The orientation of secondary cell during falling stages is similar to that of the rising stage. The difference is that the magnitudes of the flow components are larger during rising stage than that during falling stage. At section 5, the secondary flow structures and the secondary flow cells during rising and falling stages are same as of section 1 but in the opposite directions. This is because section 1 is the bend apex of the main channel while section 5 is bend apex of the main channel in opposite phase. It can be concluded that the evolution and decay processes of secondary currents during rising and falling stages are the same but only differ in strength.

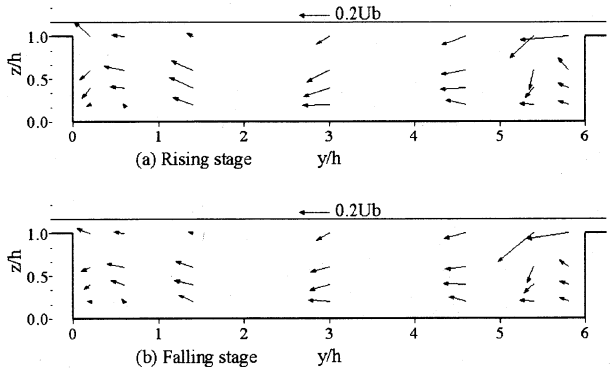

Fig. 15 Secondary currents at section 1

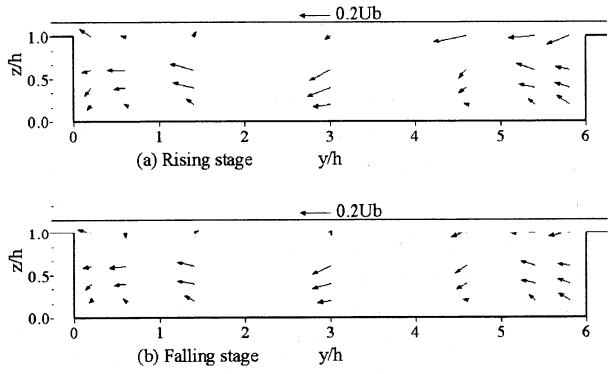

Fig. 16 Secondary currents at section 2

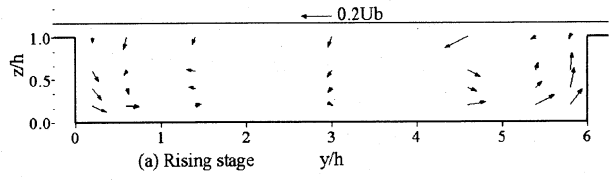

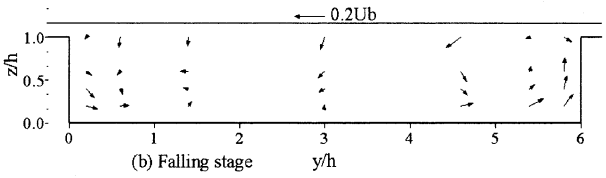

Fig. 17 Secondary currents at section 3

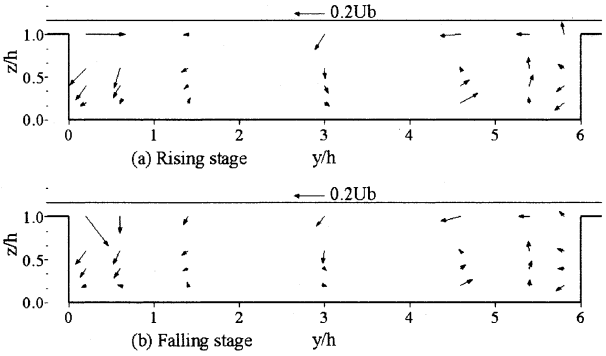

Fig. 18 Secondary currents at section 4

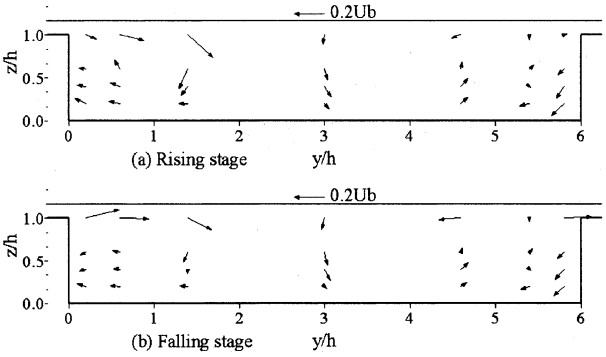

Fig. 19 Secondary currents at section 5

9. Conclusions

This paper examines the 3-D flood flow structures in terms of primary velocity distribution, stream-wise velocity distribution and secondary currents in a doubly meandering compound channel under dominant relative depth. The dominant relative depth of a doubly meandering compound channel is found be 0.17. The primary velocity distribution under the dominant relative depth appears to be essentially the same for both rising and falling stages. The position and shift of maximum and minimum primary velocity fields in the downstream direction appear to be the same for both rising and falling stages.

The stream-wise velocity pattern is the same for both rising and falling stages. The effect of the exchange of momentum between main channel and floodplain is less near the channel bottom and high at the floodplain level for both rising and falling stages. The difference in magnitude of the maximum and minimum stream-wise velocities for a particular section near main channel bed is high at the bend apex section and low at the cross-over section for both rising and falling stages. At the floodplain height, the difference in magnitudes of the maximum and minimum the stream-wise velocities is high at the cross-over section and low at the bend apex as opposed to the case near the main channel bed.

The exchange of flow between main channel and floodplain results in the retardation and deviation of flow fields. The maximum retardation occurs in the cross-over section at the floodplain level for both rising and falling stages. It is found that the extent of retardation at section 1 is higher in the rising stage than that in the falling stage while at section 3 it is higher in the falling stage than that in the rising stage. It can be seen that the angle of deviation of the stream-wise velocity is higher in the falling stage than that of the rising stage. The angle of deviation of the stream-wise velocity in the cross-over section higher in the rising stage than that of the falling stage near channel bed while it is higher in the falling stage than that of the rising stage at floodplain height. The maximum deviation occurs at the bend apex section for both rising and falling stages.

The magnitude of the secondary current under dominant relative depth can be as high as 30% of the bulk velocity. In the bend apex section, the secondary flow is dominated by the horizontal velocity component while that in the cross-over section is dominated by the vertical velocity component. The evolution and decay processes of secondary currents during rising and falling stages are essentially the same but differ in strength.

Acknowledgement

This work was supported by KAKENHI(18·06395), Grant-in-Aid for JSPS Fellows.

References

1) Knight, D.W., and Demetriou, L.D., Flood-plain and main channel flow interaction, *J. Hydraulic Engineering*, ASCE, Vol. 109, No. 8, pp. 1073-1092, 1983.
2) Wormleaton, P.R., and Merrett, D., An improved method of calculation of steady uniform flow in prismatic main/flood channel plain sections, *J. Hydraulic Research*, Vol. 28, pp. 157-174, 1990.
3) Song, T., and Graf, W.H., Velocity and turbulence distribution in unsteady open channel flow, *J. Hydraulic Engineering*, ASCE, Vol. 122, No. 3, pp. 141-154, 1996.
4) Tu, H., and Graf, W.H., Velocity Distribution in unsteady open-channel over gravel beds, *Journal of Hydroscience and Hydraulic Engineering*, JSCE, Vol. 10, No. 1, pp. 11-25, 1992.
5) Nezu, I., Nakagawa, H., Ishida, Y., and Fujimoto, H., Effects of unsteadiness on velocity profiles over rough beds in flood surface flows, *25th IAHR Congress*, Tokyo, A1, pp. 153-160, 1993.
6) Tominaga, A., Shibata, K., Mio, N., and Nagao, M., Hydraulic characteristics of unsteady flow in compound channels with wooded zone on floodplains, *Annual Journal of Hydraulic Engineering*, JSCE, Vol. 40, pp. 693-698, 1996.
7) Jayaratne, B.L., Kawahara, Y. and Kan, K., Unsteady flow characteristics in a compound channel, *27th Congress of IAHR*, San Francisco, USA, pp. 740-745, 1997.
8) Lai, C., Liu, C., and Lin., Y., Experiments on flood-wave propagation in compound channel, *J. Hydraulic Engineering*, ASCE, Vol. 126, No. 7, pp. 492-501, 2000.
9) Fukuoka, S., Watanabe, A., Okabe, H and Seki, K., Effects of unsteadiness, planform and cross-sectional form of channels on hydraulic characteristics of flood flow, *Annual Journal of Hydraulic Engineering*, JSCE, Vol. 44, pp. 867-872, 2000.
10) Morishita, Y, Uchida T, Kawahara Y, Watanabe A., Flood flow structure during rising and falling stage in a meandering compound channel, *International Conference on Civil and Environmental Engineering*, Hiroshima, pp. 287-292, 2006.
11) Graf, W.H. and Suszka, L., Unsteady flow and its effect on sediment transport, *XXI Congress of IAHR*, International Association of Hydraulic Research, 1985.
12) Islam, G.M.T., Three-dimensional flow fields in a doubly meandering compound channel under steady and unsteady flow conditions, *Ph.D. dissertation*, University of Tokyo, Japan, 2000.

(Received: April 14, 2008)